CORE
Metadata, citation and similar papers at core.ac.uk
Provided by epublications@Marquette

Marquette University
e-Publications@Marquette

Chemistry Faculty Research and Publications | Chemistry, Department of

1-1-2016

A Search for Blues Brothers: X-ray Crystallographic/Spectroscopic Characterization of the Tetraarylbenzidine Cation Radical as a Product of Aging of Solid Magic Blue

Marat R. Talipov
Marquette University

Mohammad M. Hossain
Marquette University

Anitha Boddeda
Marquette University, anitha.boddeda@marquette.edu

Khushabu Thakur
Marquette University

Rajendra Rathore
Marquette University

Accepted version. *Organic and Biomolecular Chemistry*, Vol. 14 (2016): 2961-2968. DOI. © 2016 Royal Society of Chemistry. Used with permission.

***NOT THE PUBLISHED VERSION;* this is the author's final, peer-reviewed manuscript.** The published version may be accessed by following the link in the citation at the bottom of the page.

A Search for Blues Brothers: X-Ray Crystallographic/Spectroscopic Characterization of the Tetraarylbenzidine Cation Radical as A Product of Aging of Solid Magic Blue

Marat R. Talipov
Department of Chemistry, Marquette University
Milwaukee, WI
Mohammad M. Hossain
Department of Chemistry, Marquette University
Milwaukee, WI
Anitha Boddeda
Department of Chemistry, Marquette University
Milwaukee, WI
Khushabu Thakur
Department of Chemistry, Marquette University
Milwaukee, WI
Rajendra Rathore
Department of Chemistry, Marquette University
Milwaukee, WI

Organic and Biomolecular Chemistry, Vol. 14 (2016): pg. 2961-2968. DOI. This article is © Royal Society of Chemistry and permission has been granted for this version to appear in e-Publications@Marquette. Royal Society of Chemistry does not grant permission for this article to be further copied/distributed or hosted elsewhere without the express permission from Royal Society of Chemistry.

***NOT THE PUBLISHED VERSION;* this is the author's final, peer-reviewed manuscript.** The published version may be accessed by following the link in the citation at the bottom of the page.

Magic blue (**MB**$^{+\bullet}$ $SbCl_6^-$ salt), i.e. tris-4-bromophenylamminium cation radical, is a routinely employed one-electron oxidant that slowly decomposes in the solid state upon storage to form so called 'blues brothers', which often complicate the quantitative analyses of the oxidation processes. Herein, we disclose the identity of the main 'blues brother' as the cation radical and dication of tetrakis-(4-bromophenyl)benzidine (**TAB**) by a combined DFT and experimental approach, including isolation of **TAB**$^{+\bullet}$ $SbCl_6^-$ and its X-ray crystallography characterization. The formation of **TAB** in aged magic blue samples occurs by a Scholl-type coupling of a pair of **MB** followed by a loss of molecular bromine. The recognition of this fact led us to the rational design and synthesis of tris(2-bromo-4-tert-butylphenyl)amine, referred to as 'blues cousin' (**BC**: E_{ox1} = 0.78 V vs. Fc/Fc^+, λ_{max}(**BC**$^{+\bullet}$) = 805 nm, ε_{max} = 9930 cm^{-1} M^{-1}), whose oxidative dimerization is significantly hampered by positioning the sterically demanding tert-butyl groups at the para-positions of the aryl rings. A ready two-step synthesis of **BC** from triphenylamine and the high stability of its cation radical (**BC**$^{+\bullet}$) promise that **BC** will serve as a ready replacement for **MB** and an oxidant of choice for mechanistic investigations of one-electron transfer processes in organic, inorganic, and organometallic transformations.

Introduction

Magic blue (**MB**$^{+\bullet}$ $SbCl_6^-$ salt), i.e. tris-4-bromophenylamminium cation radical,[1] is widely utilized as an aromatic oxidant for the $1e^-$ oxidation of organic, inorganic, and organometallic donors.[2–10] The popularity of the magic blue cation radical as an oxidant in part arises due to its perceived high stability, commercial availability, and reasonable oxidizing power (E_{red} = 0.70 V vs. Fc/Fc^+). With an intense and uncluttered visible absorption (λ_{max} = 728 nm, ε_{max} = 28 200 cm^{-1} M^{-1}) magic blue has also found extensive application for (quantitative) spectroscopic characterization of cation radicals and dications of organic electron donors and oxidized inorganic metal complexes and organometallic species.[11,12] Although **MB**$^{+\bullet}$ $SbCl_6^-$ salt is reasonably stable, it has been long known that **MB**$^{+\bullet}$ undergoes slow decomposition to produce impurities which have been dubbed 'blues brothers'.[2,13] During the course of our studies of organic cation radicals and dications, we observed that the presence of additional bands in

Organic and Biomolecular Chemistry, Vol. 14 (2016): pg. 2961-2968. DOI. This article is © Royal Society of Chemistry and permission has been granted for this version to appear in e-Publications@Marquette. Royal Society of Chemistry does not grant permission for this article to be further copied/distributed or hosted elsewhere without the express permission from Royal Society of Chemistry.

***NOT THE PUBLISHED VERSION;* this is the author's final, peer-reviewed manuscript.** The published version may be accessed by following the link in the citation at the bottom of the page.

the spectrum of $\mathbf{MB}^{+\bullet}$ not only interfered with spectroscopic characterization of oxidized species, but they also prevented accurate quantification of redox processes.[14]

Herein, we describe identification of the major impurity responsible for the presence of additional absorption bands in the aged samples of $\mathbf{MB}^{+\bullet}$ $SbCl_6^-$ salt as a tetraarylbenzidine cation radical/dication with the aid of electronic absorption spectroscopy, X-ray crystallography, and detailed computational studies. Moreover, the fact that the 'blues brother' in the aged $\mathbf{MB}^{+\bullet}$ sample is produced by a dimerization reaction led us to the rational synthesis of a new triarylamine derivative which prevents the dimerization reaction. This triarylamine derivative forms a stable cation radical with similar spectral properties and somewhat improved oxidizing power, and it is referred to as blues cousin, which should serve as a ready replacement for **MB** as an oxidant of choice for mechanistic investigations of one-electron transfer processes in a variety of organic, inorganic, and organometallic transformations.

Results and discussion

The initial attempt to identify the species responsible for additional absorption bands in aged samples of $\mathbf{MB}^{+\bullet}$ was carried out by its reduction using zinc dust or ferrocene, and the ^{1}H NMR analysis of the resulting neutral residue. The ^{1}H NMR analysis suggested that the sample largely contained $\mathbf{MB}^{0}$ together with a significant amount of new species and multiple other compounds in minor quantities (see Fig. S1 in the ESI†). The new species was tentatively identified by MALDI mass spectrometry to be a dimer of **MB**, which has lost a molecule of bromine, and was hypothesized to be a tetrakis-(4-bromophenyl)benzidine (Fig. S3 in the ESI†). Unfortunately, full identification of this dimer and other minor species could not be achieved because of the failure of repeated attempts of chromatographic separation.

In order to establish that additional absorption bands in the aged samples of $\mathbf{MB}^{+\bullet}$ (Fig. 1A) arise from its decomposition, we obtained an authentic spectrum of $\mathbf{MB}^{+\bullet}$ via redox titration of neutral MB using a bicyclo[2.2.1]heptane-annulated hydroquinone ether cation radical $\mathbf{THEO}^{+\bullet}$ $SbCl_6^-$ (E_{red1} = 0.67 V vs. Fc/Fc+, λ_{max} = 518 nm, ε_{max}

Organic and Biomolecular Chemistry, Vol. 14 (2016): pg. 2961-2968. DOI. This article is © Royal Society of Chemistry and permission has been granted for this version to appear in e-Publications@Marquette. Royal Society of Chemistry does not grant permission for this article to be further copied/distributed or hosted elsewhere without the express permission from Royal Society of Chemistry.

***NOT THE PUBLISHED VERSION;* this is the author's final, peer-reviewed manuscript.** The published version may be accessed by following the link in the citation at the bottom of the page.

= 7300 cm^{-1} M^{-1})[15–17] as an oxidant. The spectrum of $\mathbf{MB}^{+\bullet}$ obtained via redox titration according to Fig. 1 was found to be identical to the spectrum of the freshly prepared sample of $\mathbf{MB}^{+\bullet}$ using $\mathbf{MB}^{0}$ and $SbCl_5$ or NO^+ $SbCl_6^-$ as oxidants (Fig. 1B).

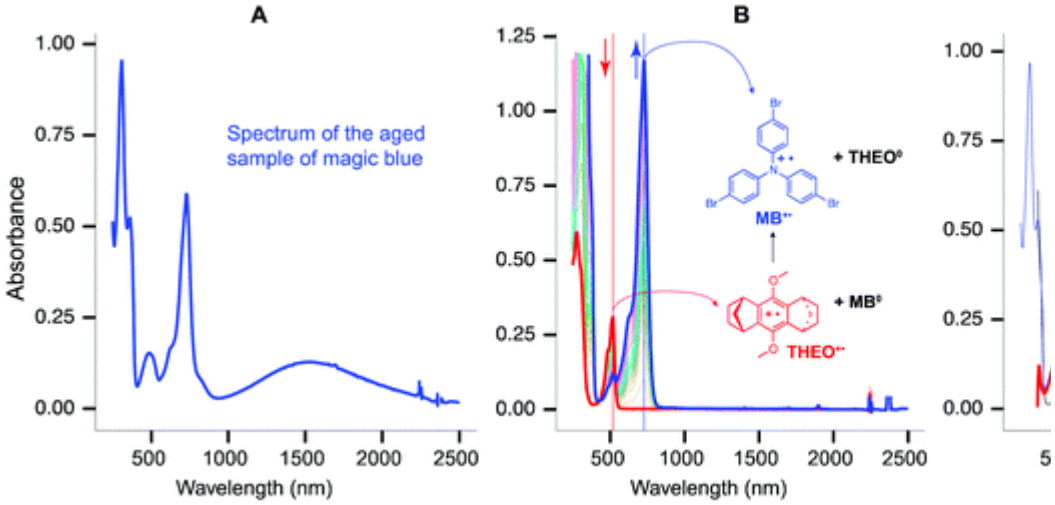

Fig. 1 (A) Absorption spectrum of the aged $\mathbf{MB}^{+\bullet}$ $SbCl_6^-$ salt at 22 °C in CH_2Cl_2; (B) spectral changes observed upon the redox titration of 42 μM $\mathbf{THEO}^{+\bullet}$ $SbCl_6^-$ with an incremental addition of 3.2 mM $\mathbf{MB}^{0}$ in CH_2Cl_2 at 22 °C; (C) spectrum obtained by the subtraction of aged $\mathbf{MB}^{+\bullet}$ (shown in panel A) and freshly prepared $\mathbf{MB}^{+\bullet}$ (shown in panel B).

A subtraction of the authentic spectrum of $\mathbf{MB}^{+\bullet}$ with that of the aged sample (~14 months old, Aldrich Chemical Co.) produced a spectrum containing bands at 480, 805, and 1550 nm (Fig. 1C), and the intensities of these bands increase with aging of the sample. The fact that these absorption bands are not attributable to pure $\mathbf{MB}^{+\bullet}$ $SbCl_6^-$ together with the presence of a low-energy transition at 1550 nm, suggested that the new absorption bands most likely arise from a cation radical and/or dication of a tetraarylbenzidine derivative.[18]

Before undertaking the synthesis of authentic samples of tetrakis(4-bromophenyl)benzidine (**TAB**) and other products arising from bromination of either **MB** or **TAB** or by intramolecular oxidative cyclization of **MB** to carbazole derivatives (see Chart 1), we first carried out (TD-)DFT calculations of all compounds in Chart 1 to obtain both redox potentials and electronic absorption spectra of their cation radicals. For this purpose, we utilized the B1LYP-40 functional [i.e.

Organic and Biomolecular Chemistry, Vol. 14 (2016): pg. 2961-2968. DOI. This article is © Royal Society of Chemistry and permission has been granted for this version to appear in e-Publications@Marquette. Royal Society of Chemistry does not grant permission for this article to be further copied/distributed or hosted elsewhere without the express permission from Royal Society of Chemistry.

***NOT THE PUBLISHED VERSION;* this is the author's final, peer-reviewed manuscript.** The published version may be accessed by following the link in the citation at the bottom of the page.

B1LYP-40/6-31G(d)+PCM(CH_2Cl_2)][19,20] because our recent careful benchmarking studies on a number of polyaromatic systems[17,20–22] showed that this functional allows an accurate description of the spin/charge (hole) distribution in their cation radicals, and, in turn, the prediction of the corresponding redox/optical properties (E_{ox1}, $\nu_{D0\rightarrow D1}$) with high fidelity to experimental data. The excellent performance of the B1LYP-40 functional owes to the fact that 40% contribution of the exact (i.e. Hartree–Fock) exchange term alleviates the self-interaction error[23,24] that causes artificial charge delocalization.

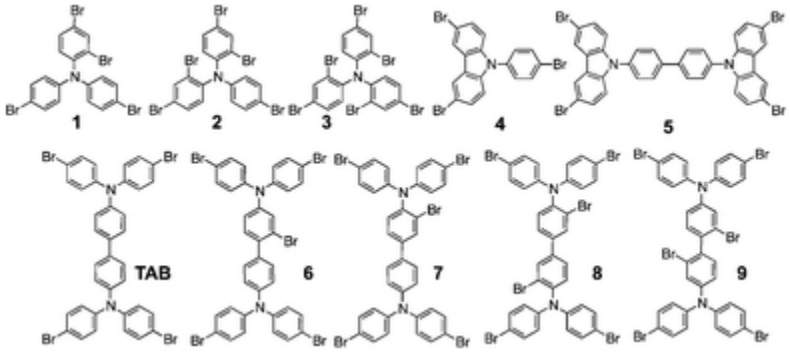

Chart 1 Possible candidates for 'blues brothers'.

The calculated equilibrium geometries of the neutral and cation radical forms of all compounds listed in Chart 1 produced their free energies of oxidation ΔG_{ox1} by a simple subtraction of the free energies of cation radicals and the corresponding neutral molecules. A plot of the computed oxidation energies (ΔG_{ox1}) against electrochemical oxidation potentials (E_{ox1}) of compounds **MB**, **1**, **2**, and **3**, available from the literature[25] (see blue diamonds and correlation line in Fig. 2), showed an excellent linear correlation that instilled confidence in our use of the B1LYP-40 functional and allowed the prediction of the oxidation potentials of various compounds in Chart 1 which are yet to be synthesized, see Table 1.

Organic and Biomolecular Chemistry, Vol. 14 (2016): pg. 2961-2968. DOI. This article is © Royal Society of Chemistry and permission has been granted for this version to appear in e-Publications@Marquette. Royal Society of Chemistry does not grant permission for this article to be further copied/distributed or hosted elsewhere without the express permission from Royal Society of Chemistry.

***NOT THE PUBLISHED VERSION;* this is the author's final, peer-reviewed manuscript.** The published version may be accessed by following the link in the citation at the bottom of the page.

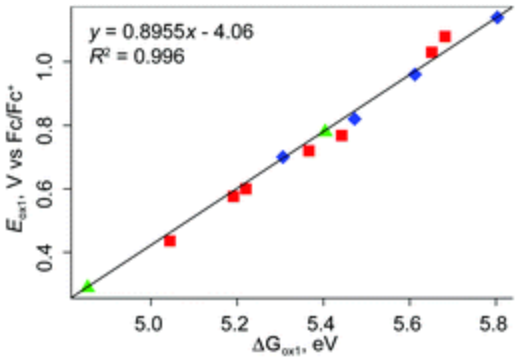

Fig. 2 A plot of experimental E_{ox1} of compounds in Chart 1 against computed ΔG_{ox1}. Note that the correlation line was generated using only **MB** and **1–3** (shown by blue diamonds) for which the electrochemical oxidation potentials were available from the literature. The red squares represent the remaining compounds in Chart 1, while the green triangles are for 'blues cousins' **10** and **BC** discussed later in the text.

Table 1 Calculated [B1LYP-40/6–31G(d) + PCM(CH_2Cl_2)] free energies of oxidation (ΔG_{ox1} and E'_{ox1}[a]) and electrochemical (E_{ox1} and E_{ox2}vs. Fc/Fc^+) oxidation potentials of various compounds in Chart 1, as well as the optical properties of their cation radicals (CRs) obtained by TD-DFT calculations ($\lambda_{D0\rightarrow D1}$ and f_{osc}) and by spectroscopic redox titration (λ_{max}(CR) and ε_{max}(CR))

Compound	ΔG_{ox1}, eV	E'_{ox1} [a], V	E_{ox1}, V	E_{ox2}, V	$\lambda_{D0\rightarrow D1}$, nm	f_{osc}	λ_{max}(CR), nm	ε_{max}(CR), M^{-1} cm^{-1}
a $E'_{ox1} = 0.8955\Delta G_{ox1} - 4.06$ (Fig. 2). b Obtained in this work by cyclic voltammetry (Fig. S4 of the ESI). c See the discussion in the text below.								
MB	5.306	0.69	0.70[25,b]	—	604	0.30	728	28 200
1	5.472	0.84	0.82[25]	—	686	0.35	757[25]	—
2	5.612	0.97	0.96[25]	—	721	0.24	805[25]	—
3	5.803	1.14	1.14[25]	—	823	0.14	880[25]	—
4	5.682	1.03	1.080[25]	—	1291	0.03	820[25]	—
5	5.651	1.00	1.030[b]	—	1526	0.27	854, 2500	—
TAB	5.044	0.46	0.436[b]	0.636[b]	1353	1.00	1490	38 100
6	5.191	0.59	0.576[b]	0.760[b]	1420	0.73	1735	24 000
7	5.220	0.61	0.600[b]	0.780[b]	1304	0.56	1750	24 500
8	5.442	0.81	0.768[b]	0.856[b]	1339	0.21	2150	15 000
9	5.366	0.75	0.720[b]	0.823[b]	1428	0.30	2128	15 000
10	4.853	0.29	0.290[b]	—	575	0.23	681	31 500
BC	5.404	0.78	0.780[b]	—	785	0.09	805	9930

The additional bands in the $\mathbf{MB^{+\bullet}}$ spectrum are expected to arise from the oxidized (i.e. cation radical or dication) forms of the blues brothers, and thus the oxidation potentials of these molecules should be lower or comparable to that of $\mathbf{MB^0}$ (i.e. 0.70 V vs. Fc/Fc^+). Accordingly, the predicted values of E'_{ox1} of various compounds in Chart 1 (Table 1) allow one to easily rule out the possibility of

Organic and Biomolecular Chemistry, Vol. 14 (2016): pg. 2961-2968. DOI. This article is © Royal Society of Chemistry and permission has been granted for this version to appear in e-Publications@Marquette. Royal Society of Chemistry does not grant permission for this article to be further copied/distributed or hosted elsewhere without the express permission from Royal Society of Chemistry.

***NOT THE PUBLISHED VERSION;* this is the author's final, peer-reviewed manuscript.** The published version may be accessed by following the link in the citation at the bottom of the page.

brominated **MB** analogues (i.e.**1–3**) and carbazole derivatives **4** and **5** as blues brothers in the spectrum of aged $\mathbf{MB}^{+\bullet}$. However, the E'_{ox1} values of $\mathbf{TAB}^{0}$ and its brominated analogues **6–9** were predicted to have lower or comparable oxidation potentials to that of $\mathbf{MB}^{0}$ and thus constitute plausible candidates for the blues brothers. In addition, TD-DFT calculations (Tables 1 and S4 in the ESI†) predict the existence of low-energy bands in the spectra of $\mathbf{TAB}^{+\bullet}$ and $\mathbf{6}^{+\bullet}$–$\mathbf{9}^{+\bullet}$, which are absent in the cation radicals of brominated **MB** analogues **1–3** and carbazole derivatives **4**.[25]

Based on the predictions from the (TD-)DFT calculations we undertook the synthesis of **TAB** and its brominated derivatives **6–9** as well as carbazole derivatives **4** and **5** using standard literature procedures,[26–36] and all synthetic details are included in the ESI.† All compounds were characterized by $^{1}H/^{13}C$ NMR spectroscopy as well as by MALDI spectrometry. These compounds were then subjected to the cyclic voltammetric analysis at 22 °C in CH_2Cl_2 containing 0.2 M tetra-n-butylammonium hexafluorophosphate at a platinum electrode. The reversible voltammograms of **TAB** and **6–9** showed two oxidation waves (Fig. S4 in the ESI†) corresponding to the formation of the cation radical and dication. The electrochemical oxidation potentials of various molecules in Chart 1 are compiled in Table 1 (columns 4 and 5), and they were in excellent agreement with the predicted oxidation potentials using DFT calculations (Table 1, column 3). Having obtained the oxidation potentials of all compounds in Chart 1, they were included in Fig. 2, and all the new points (shown as red squares) fell on the original correlation line.

We next generated the cation radicals/dications of **TAB** and **6–9** using a hindered naphthalene (i.e. 1,2,3,4,7,8,9,10-octahydro-1,1,4,4,7,7,10,10-octamethylnaphtacene) cation radical (E_{red} = 0.94 V vs. Fc/Fc^{+}, λ_{max} = 672 nm, ε_{max} = 9300 cm^{-1} M^{-1})[37,38]via redox titration under careful exclusion of moisture; see, e.g. Fig. S5 in the ESI.† The resulting absorption spectra of the cation radicals and dications of **TAB** and **6–9** are compared in Fig. 3. Interestingly, the bands contained in the absorption spectra of the cation radical and dication of **TAB** (i.e.$\mathbf{TAB}^{+\bullet}$: λ_{max} = 1490 nm, ε_{max} = 38 100 cm^{-1} M^{-1}, and λ_{max} = 489 nm, ε_{max} = 35 000 cm^{-1} M^{-1}; $\mathbf{TAB}^{2+}$: λ_{max} = 807 nm, ε_{max} = 112 600 cm^{-1} M^{-1}) closely matched the additional absorption bands in the spectrum of the aged sample of $\mathbf{MB}^{+\bullet}$, i.e. compare Fig. 3 and 1C.

Organic and Biomolecular Chemistry, Vol. 14 (2016): pg. 2961-2968. DOI. This article is © Royal Society of Chemistry and permission has been granted for this version to appear in e-Publications@Marquette. Royal Society of Chemistry does not grant permission for this article to be further copied/distributed or hosted elsewhere without the express permission from Royal Society of Chemistry.

***NOT THE PUBLISHED VERSION;* this is the author's final, peer-reviewed manuscript.** The published version may be accessed by following the link in the citation at the bottom of the page.

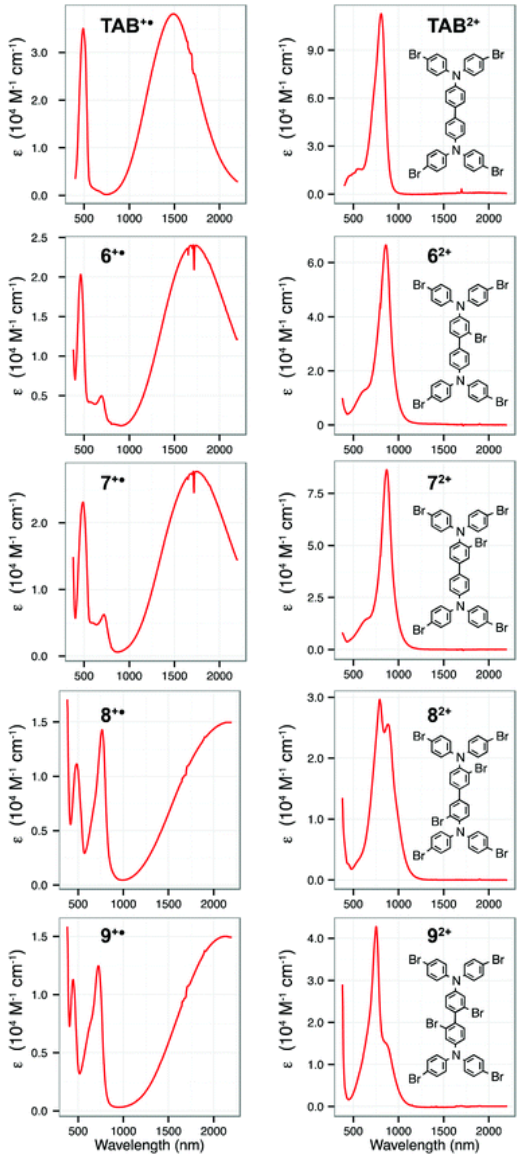

Fig. 3 Absorption spectra of cation radicals (left) and dications (right) of **TAB**, **6–9** in CH_2Cl_2 at 22 °C obtained via spectroscopic redox titrations using **THEO**$^{+\bullet}$ or **NAP**$^{+\bullet}$ (see Fig. S5 in the ESI† for the corresponding titration figures).

In order to further confirm the presence of both **TAB**$^{+\bullet}$ and **TAB**$^{2+}$ in the spectrum of the aged **MB**$^{+\bullet}$ sample, we carried out a redox titration by an incremental addition of sub-stoichiometric amounts of **TAB**^{0} to a solution of freshly prepared **MB**$^{+\bullet}$ in CH_2Cl_2 at 22 °C (Fig. 4). Interestingly, the spectrum obtained after addition of ~0.15 equivalents of **TAB**^{0} to a solution of **MB**$^{+\bullet}$ produced a spectrum which closely resembled the spectrum of the aged **MB**$^{+\bullet}$ sample

Organic and Biomolecular Chemistry, Vol. 14 (2016): pg. 2961-2968. DOI. This article is © Royal Society of Chemistry and permission has been granted for this version to appear in e-Publications@Marquette. Royal Society of Chemistry does not grant permission for this article to be further copied/distributed or hosted elsewhere without the express permission from Royal Society of Chemistry.

***NOT THE PUBLISHED VERSION;* this is the author's final, peer-reviewed manuscript.** The published version may be accessed by following the link in the citation at the bottom of the page.

(shown as thick blue line). The relative amounts of $\mathbf{TAB^{+\bullet}}$ and $\mathbf{TAB^{2+}}$ at various titration points in Fig. 4 were evaluated by a deconvolution of the individual spectra using the clean absorption spectra of $\mathbf{MB^{+\bullet}}$, $\mathbf{TAB^{+\bullet}}$, and $\mathbf{TAB^{2+}}$, which resulted in the concentrations of each species for a given titration point. This spectral deconvolution procedure allowed accurate determination of the concentrations of $\mathbf{MB^{+\bullet}}$, $\mathbf{TAB^{+\bullet}}$, and $\mathbf{TAB^{2+}}$ at every titration point in Fig. 4, and these are plotted as molar fractions against the added equivalents of $\mathbf{TAB^{0}}$ in Fig. 4B. The molar fraction vs. the added $\mathbf{TAB^{0}}$ plot clearly shows that oxidation of $\mathbf{TAB^{0}}$ by $\mathbf{MB^{+\bullet}}$, up to the equimolar concentration of $\mathbf{MB^{+\bullet}}$ and $\mathbf{TAB^{0}}$, produces both the cation radical and dication of **TAB**. Indeed, this analysis confirmed the presence of ~0.11 equivalents of $\mathbf{TAB^{+\bullet}}$ and ~0.04 equivalents of $\mathbf{TAB^{2+}}$, i.e. it amounts to the presence of ~0.15 equivalents of **TAB** in the sample of $\mathbf{MB^{+\bullet}}$ used in this study.

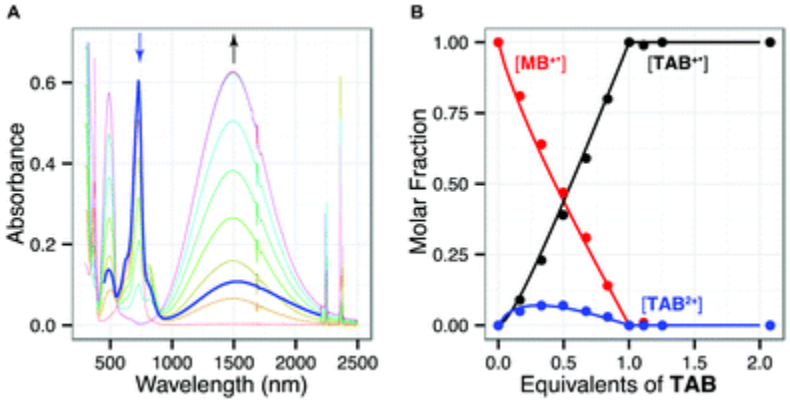

Fig. 4 (A) Spectral changes observed upon the incremental addition of 1.52 mM **TAB** to a freshly prepared solution of $\mathbf{MB^{+\bullet}}$ $SbCl_6^-$ (20 μM) in CH_2Cl_2 at 22 °C. Thick blue line shows the absorption spectrum of the aged sample of $\mathbf{MB^{+\bullet}}$ $SbCl_6^-$. (B) Molar fractions of $\mathbf{MB^{+\bullet}}$ (red circles), $\mathbf{TAB^{+\bullet}}$ (black circles), $\mathbf{TAB^{2+}}$ (blue circles) plotted against the number of added equivalents of neutral **TAB** at each addition. The data points in panel B were fitted by accounting multiple equilibria amongst various oxidized and neutral species which showed that the second oxidation potential of **TAB** is somewhat higher (E_{ox2} = 0.71 V) as compared to the electrochemical potentials (0.64 V) owing to the fact that redox titrations are carried out in the absence of an electrolyte.

The presence of **TAB** in the aged samples of $\mathbf{MB^{+\bullet}}$ was further validated by comparison of the ^{1}H NMR spectrum of the reduced $\mathbf{MB^{0}}$ with the spectrum of authentic $\mathbf{TAB^{0}}$ (Fig. S1 and S2 in the ESI†). At

Organic and Biomolecular Chemistry, Vol. 14 (2016): pg. 2961-2968. DOI. This article is © Royal Society of Chemistry and permission has been granted for this version to appear in e-Publications@Marquette. Royal Society of Chemistry does not grant permission for this article to be further copied/distributed or hosted elsewhere without the express permission from Royal Society of Chemistry.

***NOT THE PUBLISHED VERSION;* this is the author's final, peer-reviewed manuscript.** The published version may be accessed by following the link in the citation at the bottom of the page.

the same time, the ^{1}H NMR spectral analysis showed the absence of **6–9** in the aged (reduced) sample of **MB^0** (Fig. S2 in the ESI†).

Beyond its role as an impurity in the aged sample of **MB$^{+\bullet}$**, **TAB$^{+\bullet}$** represents an interesting example of a mixed-valence compound, where the DFT calculations predict that the hole was largely (88%) localized on the benzidine fragment and spread only slightly onto the p-bromophenyl rings (i.e. 3% per aryl group), as shown by the spin/charge distribution in Fig. 5 (see also Fig. S11 in the ESI†). Importantly, the 1−e$^-$ oxidation-induced bond length in **TAB**→ **TAB$^{+\bullet}$** transformation were in accordance with the disposition of the bonding/antibonding lobes of HOMO, i.e. bonds with bonding HOMO lobes undergo elongations, whereas the bonds with antibonding lobes undergo contraction, see Table S5 in the ESI.† [12,39–43] However, it is noted that HOMO density distribution in **TAB^0** is more delocalized as compared with the spin/charge distribution in **TAB$^{+\bullet}$** due to the oxidation-induced structural reorganization that involves planarization of the benzidine fragment (i.e. dihedral angle between central phenylene rings θ reduces from 35 to 19°).[17] Indeed, the HOMO density of **TAB^0** at the **TAB$^{+\bullet}$** geometry is much closer to the spin/charge density distribution in **TAB$^{+\bullet}$** (i.e. 76% on the benzidine fragment and 6% per each aryl group) than the HOMO density at the neutral **TAB** geometry (i.e. 60% on the benzidine fragment and 10% per each aryl group), see Fig. 5.

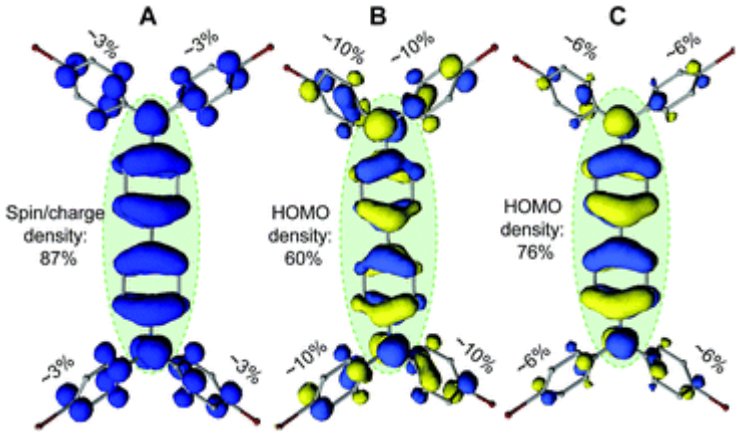

Fig. 5 (A) Spin density (0.001 au) distribution plot of **TAB$^{+\bullet}$** [B1LYP-40/6–31G(d) + PCM(CH_2Cl_2)] showing, with the aid of green ellipsoid, that 88% of spin/charge density (evaluated by the Natural Population Analysis)[44] is localized onto the benzidine fragment while the remaining 12% is evenly distributed over the four p-

Organic and Biomolecular Chemistry, Vol. 14 (2016): pg. 2961-2968. DOI. This article is © Royal Society of Chemistry and permission has been granted for this version to appear in e-Publications@Marquette. Royal Society of Chemistry does not grant permission for this article to be further copied/distributed or hosted elsewhere without the express permission from Royal Society of Chemistry.

***NOT THE PUBLISHED VERSION;* this is the author's final, peer-reviewed manuscript.** The published version may be accessed by following the link in the citation at the bottom of the page.

bromophenyl groups. (B, C) Showing the spatial distribution of HOMO of **TAB^0** and the distribution of the HOMO density [evaluated as $q_m = \Sigma_n c_{mn}^2$ where c_{mn} is the coefficient of the atomic orbital χ_{mn} in HOMO ($\varphi_{HOMO} = \Sigma_k c_k \chi_k$), m is the atomic index, and n is the index of the atomic orbital in atom m] calculated at the equilibrium geometry of neutral **TAB^0** (B) and at the equilibrium geometry of its cation radical, i.e.**TAB$^{+\bullet}$** (C).

In order to confirm this DFT prediction, we obtained single crystals of **TAB$^{+\bullet}$** $SbCl_6^-$ for crystallographic analysis. In a typical experiment, a chilled (~0 °C) Schlenk tube was charged with **TAB** (30 mg, 0.037 mmol), anhydrous CH_2Cl_2 (5 mL), and triethyloxonium hexachloroantimonate (**Et$_3$O$^+$** $SbCl_6^-$)[45] (32 mg, 0.074 mmol) under an argon atmosphere, and the resulting mixture was stirred for 30 minutes. The resulting dark-orange solution was carefully layered with dry toluene (10 mL) and placed in a refrigerator for 12 hours at −10 °C. After this time, a well-formed array of single crystals of **TAB$^{+\bullet}$** $SbCl_6^-$ was obtained and subsequently analysed by X-ray crystallography (see Fig. S8–S10 and Tables S1–S3 in the ESI†).

The ORTEP diagrams of **TAB** and **TAB$^{+\bullet}$** as well as the crystal packing diagram of **TAB$^{+\bullet}$** are presented in Fig. 6. The **TAB$^{+\bullet}$** and $SbCl_6^-$ counter ions form mixed layers along the ab plane, and within these layers, the $SbCl_6^-$ counter ions gravitate toward nitrogen atoms. The benzidine moieties are positioned in the clefts formed by the brominated aryl rings without any parallel overlap between the benzene rings, see Fig. 6D. An overlap of **TAB** and **TAB$^{+\bullet}$** structures clearly shows that the benzidine fragment of **TAB** is significantly planarized (i.e., the value of θ decreased from 22° to 3°) while the p-bromophenyl rings become much more propeller-shaped (i.e. reduced conjugation with nitrogen lone pairs as judged by change in the average dihedral angle from ~45° to ~35°) upon 1e$^-$ oxidation.

Organic and Biomolecular Chemistry, Vol. 14 (2016): pg. 2961-2968. DOI. This article is © Royal Society of Chemistry and permission has been granted for this version to appear in e-Publications@Marquette. Royal Society of Chemistry does not grant permission for this article to be further copied/distributed or hosted elsewhere without the express permission from Royal Society of Chemistry.

***NOT THE PUBLISHED VERSION;* this is the author's final, peer-reviewed manuscript.** The published version may be accessed by following the link in the citation at the bottom of the page.

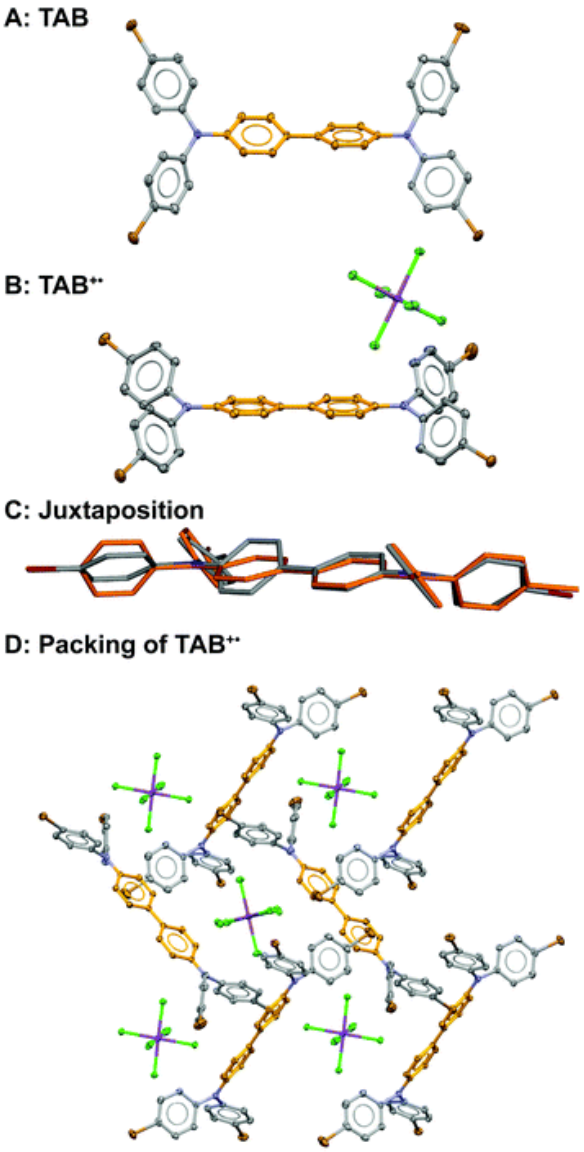

Fig. 6 The ORTEP diagrams (50% probability) of **TAB^{0}** (A) and **TAB$^{+\bullet}$** $SbCl_6^-$ (B) as well as the juxtaposition of **TAB^{0}** (grey color) and **TAB$^{+\bullet}$** (orange color) showing planarization of the benzidine fragment and enhanced propeller arrangement of the p-bromophenyl groups around the nitrogen atoms (C). The packing arrangement of **TAB$^{+\bullet}$** $SbCl_6^-$ showing the layers of **TAB** units with no close contact between the benzidine fragments, which are separated by the $SbCl_6^-$ counter anions (D). Note that the co-crystallized CH_2Cl_2 molecules and hydrogens were omitted for clarity. Also see Fig. S8–S10 and Tables S1–S3 in the ESI.†

Availability of precise X-ray structures of **TAB$^{+\bullet}$** $SbCl_6^-$ as well as of neutral **TAB** allowed a comparison of the bond length changes in the **TAB**→ **TAB$^{+\bullet}$** transformation. Expectedly, the bond contractions and elongations were mostly confined to the benzidine fragment of

Organic and Biomolecular Chemistry, Vol. 14 (2016): pg. 2961-2968. DOI. This article is © Royal Society of Chemistry and permission has been granted for this version to appear in e-Publications@Marquette. Royal Society of Chemistry does not grant permission for this article to be further copied/distributed or hosted elsewhere without the express permission from Royal Society of Chemistry.

***NOT THE PUBLISHED VERSION;* this is the author's final, peer-reviewed manuscript.** The published version may be accessed by following the link in the citation at the bottom of the page.

TAB, which was significantly planarized (i.e., the value of θ decreased from 22° to 3°) upon 1e⁻ oxidation, while the four p-bromophenyl rings did not undergo significant bond length changes (Fig. 7). Moreover, a comparison of the bond length changes in **TAB**→ **TAB**$^{+\bullet}$ transformation by DFT calculations and X-ray structural analysis clearly shows a linear correspondence (Fig. 7), and thus confirming the validity of the usage of B1LYP-40 functional for DFT calculations.

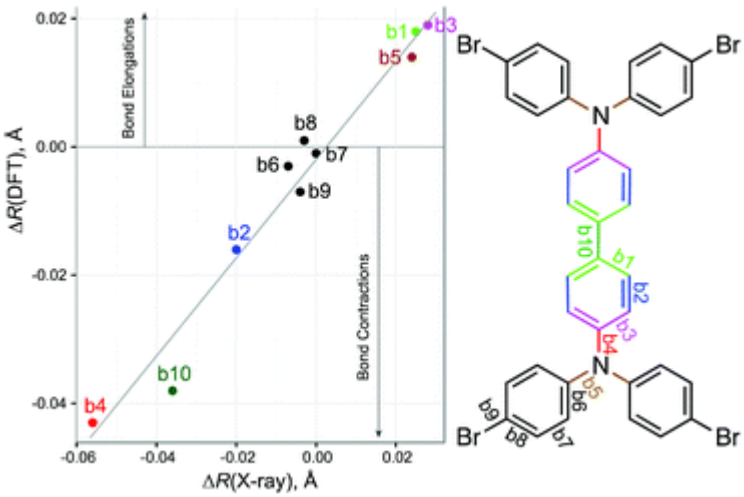

Fig. 7 Comparison of the oxidation-induced bond length changes (in Å) in **TAB** obtained by X-ray crystallography (abscissa) and DFT calculations (ordinate). Note that the bond length changes (i.e. b1–b10) depicted in the structure are based on the averages of equivalent bonds. See also Fig. S12 and Table S5 in the ESI.†

These results clearly suggest that spectral contamination in the aged sample of **MB**$^{+\bullet}$ is largely due to the formation of **TAB**$^{+\bullet}$ and **TAB**$^{2+}$, which most likely are produced by the oxidative Scholl-type reaction,[46] where an eventual loss of a molecular bromine produces **TAB**, which undergoes oxidation with **MB**$^{+\bullet}$.[47] To prevent degradation of **MB**$^{+\bullet}$, we propose to substitute bromine atoms in the para-positions of **MB** by the sterically demanding tertiary-butyl groups, and place bromine atoms at ortho-positions of the aromatic ring (see Scheme 1). The synthesis of the proposed tris(2-bromo-4-^{t}butylphenyl)amine (**BC**) was easily accomplished from readily available triphenylamine by a facile t-butylation[48] using t-butanol and trifluoroacetic acid followed by bromination using NBS in DMF (see Scheme S8 in the ESI† for details).

Organic and Biomolecular Chemistry, Vol. 14 (2016): pg. 2961-2968. DOI. This article is © Royal Society of Chemistry and permission has been granted for this version to appear in e-Publications@Marquette. Royal Society of Chemistry does not grant permission for this article to be further copied/distributed or hosted elsewhere without the express permission from Royal Society of Chemistry.

***NOT THE PUBLISHED VERSION;* this is the author's final, peer-reviewed manuscript.** The published version may be accessed by following the link in the citation at the bottom of the page.

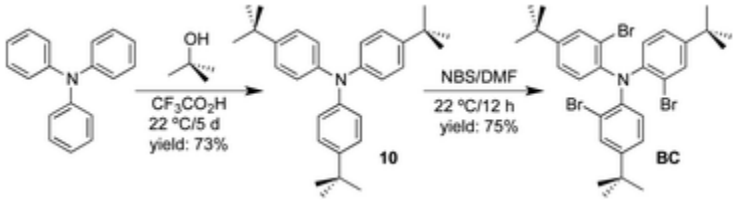

Scheme 1 Synthesis of BC.

Cyclic voltammetric analysis of tris(4-^{t}butylphenyl)amine (**10**) and its brominated analogue **BC** (Fig. 8A and S7 in the ESI†) showed that they undergo reversible one-electron oxidation at varying scan rates (v = 50 to 300 mV s^{-1}). Interestingly, a placement of bromine atoms at the ortho-positions in **10** increases its oxidation potential from 0.29 to 0.78 V vs. Fc/Fc^+, which suggests that 'blues cousin' has slightly higher oxidizing power [i.e. $E_{red}(\mathbf{BC}^{+\bullet})$ = 0.78 V] as compared to 'magic blue' [i.e. $E_{red}(\mathbf{MB}^{+\bullet})$ = 0.70 V].

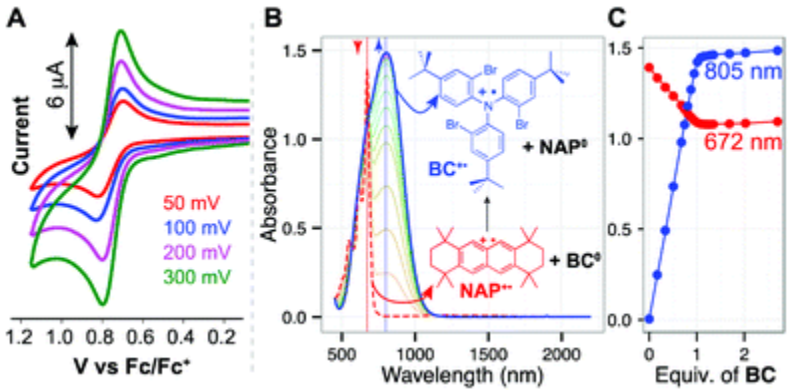

Fig. 8 (A) Cyclic voltammograms of 5 mM **BC** in CH_2Cl_2 (22 °C) containing 0.2 M tetra-n-butylammonium hexafluorophosphate at different scan rates (as denoted). (B) Spectral changes attendant upon incremental addition of 3.0 mM $\mathbf{BC}^{0}$ to a solution of $\mathbf{NAP}^{+\bullet}$ $SbCl_6^-$ (0.15 mM) in CH_2Cl_2 at 22 °C (see also Fig. S6 in the ESI†), and (C) plot of decrease of absorbance at 672 nm (due to the disappearance of $\mathbf{NAP}^{+\bullet}$) and increase of absorbance at 805 nm (due to the formation of $\mathbf{BC}^{+\bullet}$) against the equivalents of added neutral $\mathbf{BC}^{0}$.

The cation radical of **BC** was first generated by the spectroscopic redox titration, where sub-stoichiometric amounts of $\mathbf{BC}^{0}$ were incrementally added to a solution of $\mathbf{NAP}^{+\bullet}$ (Fig. 8). The absorption spectrum of $\mathbf{BC}^{+\bullet}$ showed a low-energy band at λ_{max} = 805 nm (ε_{max} = 9930 cm^{-1} M^{-1}) which is slightly red-shifted as compared

Organic and Biomolecular Chemistry, Vol. 14 (2016): pg. 2961-2968. DOI. This article is © Royal Society of Chemistry and permission has been granted for this version to appear in e-Publications@Marquette. Royal Society of Chemistry does not grant permission for this article to be further copied/distributed or hosted elsewhere without the express permission from Royal Society of Chemistry.

***NOT THE PUBLISHED VERSION;* this is the author's final, peer-reviewed manuscript.** The published version may be accessed by following the link in the citation at the bottom of the page.

to the absorption band of $\mathbf{MB}^{+\bullet}$ (λ_{max} = 728 nm, ε_{max} = 28 200 cm^{-1} M^{-1}). Note that $\mathbf{BC}^{+\bullet}$ $SbCl_6^-$ can be prepared as a crystalline solid either by reaction with $SbCl_5$ or NO^+ $SbCl_6^-$ similar to the preparation of $\mathbf{MB}^{+\bullet}$ $SbCl_6^-$ (see ESI†), and the spectrum of the resulting $\mathbf{BC}^{+\bullet}$ was identical to the spectrum presented in Fig. 8B.

The high stability of $\mathbf{BC}^{+\bullet}$ $SbCl_6^-$ will allow it to serve as a convenient replacement of $\mathbf{MB}^{+\bullet}$ $SbCl_6^-$, and we believe that it will find widespread use for the spectroscopic characterization of various oxidized species, and will become a useful chemical oxidant for various oxidative transformations.

Conclusions

In summary, we have demonstrated that 'magic blue' ($\mathbf{MB}^{+\bullet}$) undergoes slow decomposition in the solid state upon aging thus giving rise to the additional absorption bands at 480 nm, 805 nm, and 1550 nm. A combined DFT and experimental (NMR, electrochemistry, optical spectroscopy, and X-ray crystallography) study led to the identification of the main decomposition product, or blues brother, as tetrakis-(4-bromophenyl)benzidine whose cation radical (λ_{max} = 489, 1490 nm) and dication (807 nm) are responsible for the additional absorption bands.

This study allowed us to further demonstrate the excellent performance of the B1LYP-40 functional for accurately predicting the electrochemical oxidation potentials of a variety of triarylamine derivatives and the optical properties of their cation radicals by (TD-)DFT calculations which aided in identification of the blues brother. Moreover, the excellent performance of the B1LYP-40 functional[17,19–22] was further demonstrated by close correspondence of the calculated structures of **TAB** and $\mathbf{TAB}^{+\bullet}$ with those obtained by X-ray crystallography.

The fact that **TAB** is formed by dimerization of **MB** led us to design and synthesize its close analogue tris(2-bromo-4-tert-butylphenyl)amine referred to as 'blues cousin' (**BC**: E_{ox1} = 0.78 V vs. Fc/Fc^+, $\lambda_{max}(\mathbf{BC}^{+\bullet})$ = 805 nm, ε_{max} = 9930 cm^{-1} M^{-1}), in which oxidative dimerization is hampered by positioning the sterically demanding tert-butyl groups at the para-positions of the aryl rings.

Organic and Biomolecular Chemistry, Vol. 14 (2016): pg. 2961-2968. DOI. This article is © Royal Society of Chemistry and permission has been granted for this version to appear in e-Publications@Marquette. Royal Society of Chemistry does not grant permission for this article to be further copied/distributed or hosted elsewhere without the express permission from Royal Society of Chemistry.

***NOT THE PUBLISHED VERSION;* this is the author's final, peer-reviewed manuscript.** The published version may be accessed by following the link in the citation at the bottom of the page.

The ease of preparation of **BC^0** and high stability of its cation radical (**BC$^{+\bullet}$**) suggest that it will become a useful one-electron oxidant for widespread use in organic, organometallic, and inorganic chemistry.

Acknowledgements

We thank the NSF (CHE-1508677) and NIH (R01-HL112639–04) for financial support and Dr Sergey V. Lindeman for X-ray crystallography. The calculations were performed on the high-performance computing cluster Père at Marquette University funded by NSF awards OCI-0923037 and CBET-0521602, and the Extreme Science and Engineering Discovery Environment (XSEDE) funded by NSF (TG-CHE130101).

References

1. F. A. Bell, A. Ledwith and D. C. Sherrington, J. Chem. Soc. C, 1969, 2719–2720.
2. N. G. Connelly and W. E. Geiger, Chem. Rev., 1996, 96, 877–910.
3. K. T. Lorenz and N. L. Bauld, J. Am. Chem. Soc., 1987, 109, 1157–1160.
4. T. Kim, G. A. Mirafzal, J. Liu and N. L. Bauld, J. Am. Chem. Soc., 1993, 115, 7653–7664.
5. A. M. Bond, R. Colton, D. A. Fiedler, J. E. Kevekordes, V. Tedesco and T. F. Mann, Inorg. Chem., 1994, 33, 5761–5766.
6. W. Yueh and N. L. Bauld, J. Am. Chem. Soc., 1995, 117, 5671–5676.
7. N. L. Bauld, J. T. Aplin, W. Yueh, H. Sarker and D. J. Bellville, Macromolecules, 1996, 29, 3661–3662.
8. K. Heinze and S. Reinhardt, Organometallics, 2007, 26, 5406–5414.
9. H. Wang, X. Wang, M. A. Winnik and I. Manners, J. Am. Chem. Soc., 2008, 130, 12921–12930.
10. C. M. Davis, K. Ohkubo, I.-T. Ho, Z. Zhang, M. Ishida, Y. Fang, V. M. Lynch, K. M. Kadish, J. L. Sessler and S. Fukuzumi, Chem. Commun., 2015, 51, 6757–6760.
11. R. Rathore and C. L. Burns, J. Org. Chem., 2003, 68, 4071–4074.
12. T. S. Navale, L. Zhai, S. V. Lindeman and R. Rathore, Chem. Commun., 2009, 2857–2859.

Organic and Biomolecular Chemistry, Vol. 14 (2016): pg. 2961-2968. DOI. This article is © Royal Society of Chemistry and permission has been granted for this version to appear in e-Publications@Marquette. Royal Society of Chemistry does not grant permission for this article to be further copied/distributed or hosted elsewhere without the express permission from Royal Society of Chemistry.

***NOT THE PUBLISHED VERSION;* this is the author's final, peer-reviewed manuscript.** The published version may be accessed by following the link in the citation at the bottom of the page.

13. L. Eberson and B. Larsson, Acta Chem. Scand., 1986, 40, 210–225.
14. R. Rathore, S. V. Lindeman, A. S. Kumar and J. K. Kochi, J. Am. Chem. Soc., 1998, 120, 6931–6939.
15. R. Rathore and J. K. Kochi, J. Org. Chem., 1995, 60, 4399–4411.
16. R. Rathore, C. L. Burns and M. I. Deselnicu, Org. Synth., 2005, 1–9.
17. M. R. Talipov, A. Boddeda, S. V. Lindeman and R. Rathore, J. Phys. Chem. Lett., 2015, 6, 3373–3378.
18. K. Sreenath, C. V. Suneesh, V. K. R. Kumar and K. R. Gopidas, J. Org. Chem., 2008, 73, 3245–3251.
19. M. Renz, K. Theilacker, C. Lambert and M. Kaupp, J. Am. Chem. Soc., 2009, 131, 16292–16302.
20. M. R. Talipov, A. Boddeda, Q. K. Timerghazin and R. Rathore, J. Phys. Chem. C, 2014, 118, 21400–21408.
21. M. R. Talipov, T. S. Navale and R. Rathore, Angew. Chem., Int. Ed., 2015, 54, 14468–14472.
22. M. R. Talipov, R. Jasti and R. Rathore, J. Am. Chem. Soc., 2015, 137, 14999–15006.
23. A. J. Cohen, P. Mori-Sánchez and W. Yang, Science, 2008, 321, 792–794.
24. A. J. Cohen, P. Mori-Sánchez and W. Yang, Chem. Rev., 2011, 112, 289–320.
25. W. S. E. Steckhan and W. Schmidt, Chem. Ber., 1980, 113, 577–585.
26. H. R. Snyder, C. Weaver and C. D. Marshall, J. Am. Chem. Soc., 1949, 71, 289–291.
27. R. Belcher, A. J. Nutten and W. I. Stephen, J. Chem. Soc., 1958, 2336–2338.
28. J. Cornforth, R. H. Cornforth and R. T. Gray, J. Chem. Soc., Perkin. Trans. 1, 1982, 2289–2297.
29. H.-M. Kang, Y.-K. Lim, I.-J. Shin, H.-Y. Kim and C.-G. Cho, Org. Lett., 2006, 8, 2047–2050.
30. N. Berton, I. Fabre-Francke, D. Bourrat, F. Chandezon and S. Sadki, J. Phys. Chem. B, 2009, 113, 14087–14093.
31. J. Vicente, J. Gil-Rubio, G. Zhou, H. J. Bolink and J. Arias-Pardilla, J. Polym. Sci., Part A: Polym. Chem., 2010, 48, 3744–3757.

Organic and Biomolecular Chemistry, Vol. 14 (2016): pg. 2961-2968. DOI. This article is © Royal Society of Chemistry and permission has been granted for this version to appear in e-Publications@Marquette. Royal Society of Chemistry does not grant permission for this article to be further copied/distributed or hosted elsewhere without the express permission from Royal Society of Chemistry.

***NOT THE PUBLISHED VERSION;* this is the author's final, peer-reviewed manuscript.** The published version may be accessed by following the link in the citation at the bottom of the page.

32. J. H. Cho, Y.-S. Ryu, S. H. Oh, J. K. Kwon and E. K. Yum, Bull. Korean Chem. Soc., 2011, 32, 2461.
33. M. Wang, C. Li, A. Lv, Z. Wang, Z. Bo and F. Zhang, Polymer, 2012, 53, 324–332.
34. H.-F. Huang, S.-H. Xu, Y.-B. He, C.-C. Zhu, H.-L. Fan, X.-H. Zhou, X.-C. Gao and Y.-F. Dai, Dyes Pig., 2013, 96, 705–713.
35. B.-Y. Lim, B.-E. Jung and C.-G. Cho, Org. Lett., 2014, 16, 4492–4495.
36. J. Safaei-Ghomi and Z. Akbarzadeh, Ultrason. Sonochem., 2015, 22, 365–370.
37. R. Rathore and J. K. Kochi, Acta Chem. Scand., 1998, 52, 114–130.
38. R. Rathore, C. L. Burns and M. I. Deselnicu, Org. Lett., 2001, 3, 2887–2890.
39. M. Banerjee, V. S. Vyas, S. V. Lindeman and R. Rathore, Chem. Commun., 2008, 1889–1891.
40. R. Shukla, S. H. Wadumethrige, S. V. Lindeman and R. Rathore, Org. Lett., 2008, 10, 3587–3590.
41. V. J. Chebny, T. S. Navale, R. Shukla, S. V. Lindeman and R. Rathore, Org. Lett., 2009, 11, 2253–2256.
42. V. J. Chebny, R. Shukla, S. V. Lindeman and R. Rathore, Org. Lett., 2009, 11, 1939–1942.
43. T. S. Navale, K. Thakur, V. S. Vyas, S. H. Wadumethrige, R. Shukla, S. V. Lindeman and R. Rathore, Langmuir, 2012, 28, 71–83.
44. F. Weinhold and C. R. Landis, Valency and bonding: a natural bond orbital donor–acceptor perspective, Cambridge University Press, Cambridge, New York, UK, 2005.
45. R. Rathore, A. S. Kumar, S. V. Lindeman and J. K. Kochi, J. Org. Chem., 1998, 63, 5847–5856.
46. L. Zhai, R. Shukla, S. H. Wadumethrige and R. Rathore, J. Org. Chem., 2010, 75, 4748–4760.
47. Magic blue is rather stable and does not undergo ready dimerization, and therefore it is likely that a slow decomposition of **MB**$^{+\bullet}$ to neutral **MB** catalyses the formation of **TAB**. For example, see: O. Yurchenko, D. Freytag, L. zur Borg, R. Zentel, J. Heinze and S. Ludwigs, J. Phys. Chem. B, 2012, 116, 30–39 and M. Talipov and R. Rathore, Robust Aromatic Cation Radicals as Redox Tunable Oxidants, in Organic Redox Systems:

Organic and Biomolecular Chemistry, Vol. 14 (2016): pg. 2961-2968. DOI. This article is © Royal Society of Chemistry and permission has been granted for this version to appear in e-Publications@Marquette. Royal Society of Chemistry does not grant permission for this article to be further copied/distributed or hosted elsewhere without the express permission from Royal Society of Chemistry.

***NOT THE PUBLISHED VERSION;* this is the author's final, peer-reviewed manuscript.** The published version may be accessed by following the link in the citation at the bottom of the page.

Synthesis, Properties, and Applications, ed. T. Nishinaga, John Wiley & Sons, Inc, Hoboken, NJ, 2015, pp. 131–175.

48. D. Vak, J. Jo, J. Ghim, C. Chun, B. Lim, A. J. Heeger and D.-Y. Kim, Macromolecules, 2006, 39, 6433–6439.

Footnote

† Electronic supplementary information (ESI) available: Details of synthesis and characterization data for various compounds including cyclic voltammetry, generation of cation radicals, X-ray crystallography, and computational details. CCDC 1445500, 1445501 and 1445573. For ESI and crystallographic data in CIF or other electronic format see DOI: 10.1039/c6ob00140h

Organic and Biomolecular Chemistry, Vol. 14 (2016): pg. 2961-2968. DOI. This article is © Royal Society of Chemistry and permission has been granted for this version to appear in e-Publications@Marquette. Royal Society of Chemistry does not grant permission for this article to be further copied/distributed or hosted elsewhere without the express permission from Royal Society of Chemistry.